

Theoretical Study on the Grafting Reaction of Maleimide Containing 2-Hydroxy-Benzophenone Onto Polyethylene

hui Zhang (✉ hust_zhanghui11@hotmail.com)

Harbin University of Science and Technology

Chi Deng

Harbin University of Science and Technology

Xia Du

Harbin University of Science and Technology

Yan Shang

Harbin University of Science and Technology

Hong Zhao

Harbin University of Science and Technology

Xuan Wang

Harbin University of Science and Technology

Baozhong Han

Harbin University of Science and Technology

Zesheng Li

Harbin University of Science and Technology

Research Article

Keywords: Cross-linked Polyethylene, Maleimide, Benzophenone, Transition states

Posted Date: May 10th, 2021

DOI: <https://doi.org/10.21203/rs.3.rs-478525/v1>

License: © ⓘ This work is licensed under a Creative Commons Attribution 4.0 International License.

[Read Full License](#)

Version of Record: A version of this preprint was published at Journal of Molecular Modeling on August 20th, 2021. See the published version at <https://doi.org/10.1007/s00894-021-04874-2>.

1 Theoretical Study on the Grafting Reaction of Maleimide Containing 2 2-Hydroxy-Benzophenone onto Polyethylene

3 Hui Zhang^{a,1}, Chi Deng^a, Xia Du^a, Yan Shang^a, Hong Zhao^{a,2}, Xuan Wang^a,
4 Baozhong Han^{a,b,3}, Zesheng Li^c

5 ^aKey Laboratory of Engineering Dielectrics and Its Application of Ministry of Education & School
6 of Material Science & Engineering, Harbin University of Science and Technology, Harbin
7 150080, P.R. China;

8 ^bShanghai Qifan Cable Co., Ltd., Shanghai 200008, P.R. China

9 ^cKey Laboratory of Cluster Science of Ministry of Education & School of Chemistry, Beijing
10 Institute of Technology, Beijing 100081, P.R. China;

11 **Abstract:** A theoretical study on the multi-channel hydrogen addition of maleimide
12 containing 2-hydroxy-benzophenone onto polyethylene in Ultra-Violet (UV) radiation
13 cross-linking process was carried out using density functional theory (DFT) method at
14 the B3LYP/6-311+G(d,p) level. The energetic information and the minimum energy
15 path (MEP) are calculated of nine reaction channels. The electrophilic addition
16 reactions at two positions in the target molecule (maleimide containing
17 2-hydroxy-benzophenone) were investigated, where are on the C atom of C=C groups
18 and on the O atom of C=O groups. Frontier MOs and NBO charge population of the
19 target molecule have been analyzed in detail. As a result, the reaction site of C in C=C
20 group is more active than the site of O in C=O groups. The target molecule can be
21 used as a multi-functional additive candidate. The predicted mechanism may provide
22 a theoretical basis for the real application of XLPE high voltage insulation cables.

23 **Keywords:** Cross-linked Polyethylene; Maleimide; Benzophenone; Transition states
24

¹Corresponding author e-mail: hust_zhanghui11@hotmail.com

²Corresponding author e-mail: hongzhao@hrbust.edu.cn

³Corresponding author e-mail: hbzhlj@163.com

25 **Introduction**

26 Cross-linked polyethylene (XLPE) insulation cables have broad application prospects
27 in high voltage and ultra-high voltage fields due to the superiority of their electrical
28 performance [1]. The insulation material is one of the most important issues for
29 restricting the fast development of polymeric high voltage direct current (HVDC)
30 cables in the near future. The electrical treeing and the space charge accumulation
31 leads to decreasing of service behavior in-service XLPE cables [2-5]. Hence, voltage
32 stabilizer and space charge inhibitor are needed to increase the electric breakdown
33 strength and inhibit space charge accumulation in the polyethylene (PE) insulation
34 materials. Voltage stabilizers can effectively improve the electrical treeing resistance,
35 which usually have polycyclic aromatic hydrocarbons structure [6-11]. Our group
36 proposes a guiding criterion using the electron affinity and the reaction potential
37 barrier heights to identify high efficiency of the voltage stabilizers [5-7]. And it is
38 reported that polar molecules (such as maleic anhydride) can be grafted to the
39 polymer chains with the aim of inducing deep traps and reducing the accumulation of
40 space charge [12,13]. Our group also proposes a guiding criterion using the reaction
41 potential barrier heights to identify high efficiency of the space charge inhibitor
42 [14-15].

43 Compared with the traditional dicumyl peroxide (DCP) crosslinking technology,
44 Ultra-Violet (UV) radiation crosslinking technology has become a candidate because
45 of its advantages such as fast processing speed, small radiation area, energy saving
46 and insensitive to heat. And theoretical studies [16-17] also show that the reaction
47 energy barrier of hydrogen abstraction on the PE chain by benzophenone (BP) is 0.17
48 eV in the UV radiation cross-linking process, which is 0.08 eV lower than 0.25 eV for
49 the hydrogen abstraction on the PE chain by the cumyl peroxide (CP) radical in DCP

50 cross-linking process. This indicates that UV radiation cross-linking process has the
51 advantage of replacing traditional DCP process for XLPE production.

52 Recently, Kim's group [18] reported the reaction conditions and photo-stabilization
53 effects of the synthesized novel UV absorber (abbreviated as **AB**, a benzoic acid
54 derivative containing maleimide group and 2-hydroxy-benzophenone group). As an
55 effective light stabilizer, UV absorber is widely used to assimilate UV light with short
56 wavelength (200-400 nm) and convert it into harmless form. This give us an
57 inspiration, can the **AB** be used as a multi-functional additive to improve the voltage
58 stabilization and space charge inhibition property of insulation materials? Molecular
59 structure of the **AB** is presented in Fig.1. The name and abbreviation of the studied
60 molecules are listed in Table 1. We expect the carbonyl group or benzene in **AB**
61 molecule to act as deep traps to inhibit space charge and meanwhile it can be used as a
62 voltage stabilizer to improve electrical tree resistance capability. The addition of the
63 multi-functional **AB** in system would decrease the amount of additive to reduce the
64 introduction of chemical impurities, the electronic conductivity of the materials will
65 reduce.

66 In this paper, 4-methylheptane (Pe) was selected as model molecule of PE, we further
67 clarify and verify the possibility of the **AB** used as a potential multi-functional
68 additive with the capability of capturing electrons. There are three issues need to be
69 solved. (1) Whether the **AB** can be sensitized to triplet state with the help of initiator
70 BP? (2) Which sites of addition reaction on the **AB** is more reactive, double bond
71 addition or carbonyl hydrogen addition? (3) Which reaction channel should be the
72 dominant one among four hydrogen addition sites in **AB** molecule?

73 Clarifying the reaction mechanism is beneficial to optimize the crosslinking process
74 of UV radiation and promote the development of high voltage cable insulation

75 materials.

76 **2. Computational Methods**

77 In this work, the geometry optimizations and frequency calculations of all the
78 stationary points on the ground state S_0 or the triplet state T_1 were carried out by DFT
79 method [19] at the B3LYP [20-23] functional level with the 6-311+G(*d,p*) basis set.
80 The minimum energy path (MEP) is calculated at the same level and obtained by the
81 intrinsic reaction coordinate (IRC) theory. The gradient step is 0.05 (amu)^{1/2} Bohr.
82 Based on these electronic structure calculations, we obtain the values of E_g , IP(*a*) and
83 EA(*a*), respectively. E_g refers to the energy gaps between the highest occupied
84 molecular orbital (HOMO) and the lowest unoccupied molecular orbital (LUMO),
85 IP(*a*) refers to the adiabatic ionization potentials and EA(*a*) refers to the adiabatic
86 electron affinities. Based on the optimized geometries, we calculate the lowest triplet
87 excitation energies (T_1) of the studied molecules by the time-dependent density
88 functional theory (TDDFT) method [24,25]. The natural charge population was
89 analyzed by the natural bond orbital (NBO) method [26]. All the electronic structure
90 calculations were performed by the GAUSSIAN09 program package [27].

91 **3. Results and Discussion**

92 The calculated lowest triplet excitation energies (T_1) of **AB** (0.10 eV) in this work is
93 much lower than that of the photo-initiator BP (0.73 eV) [15] at the
94 B3LYP/6-311+G(*d,p*) level by the TDDFT method [24,25]. In the process of UV
95 radiation, BP will be excited from S_0 to its singlet excited state S_1 (n, π^*) and after to
96 its triplet excited state T_1 (n, π^*) through inter system crossing (ISC). According to the
97 sensitization rule, **AB** molecule will be sensitized to its T_1 state by BP because the
98 excitation energies of T_1 state is 0.63 eV lower than that of BP. That is to say, the T_1
99 state Bp quenches by the S_0 state **AB**, forming the T_1 state **AB** and the S_0 state BP. **AB**

100 can be grafted onto the PE chain, which consists of two fragments,
101 4-(2,5-dioxo-2,5-dihydro-pyrrol-1-yl)- benzoic acid (**A** fragment) and
102 2,4-dihydroxybenzophenone (**B** fragment) [18]. We calculated key structural
103 parameters of the reactions between the molecule **AB** and the model compound Pe are
104 listed in Table 2. At the same time, the relevant data of the two fragments **A** and **B** are
105 also listed in Table 2. The E_g , $IP(a)$ s, and $EA(a)$ s of studied molecules calculated are
106 listed in Table 3, and their NBO calculation results are listed in Table 4.

107 *3.1. Stationary point geometries and NBO Charge Population*

108 The optimized structures of the reactants, transition states and products on S_0 or T_1
109 states for nine channels were obtained. The standard coordination of the TSs for every
110 channel is given in the supporting information. The schematic diagram of reaction
111 progress of the studied nine channels is shown in Fig. 2.

112 Four sites on the **AB** molecule can undergo H addition reactions with Pe, one is
113 electrophilic addition reaction of the 4-position hydrogen in Pe to C of C=C group
114 and the other three are electrophilic addition reaction of the 4-position hydrogen in Pe
115 to O of C=O groups (the three sites are carbonyl in amide, ester carbonyl and ketone
116 carbonyl, respectively). The natural charge density (-0.14) on site 1 in AB molecule
117 given in Table 4 is lower than that of others.

118 The maleimide structure in Fig. 1, the N atom and the carbonyl group C=O form p- π
119 conjugate, and N atom exhibits a strong electron donating conjugation effect, which
120 increases the electron cloud density on the carbonyl group C=O, and the π electron
121 cloud shifts from C to O, which increases the amount of negative charge on O of C=O
122 (site 2). As a result, the density of the electron cloud on the C=C double bond
123 decreases significantly. The electrophilic addition reaction of C=C group in the **AB**
124 molecule would be easier than that of C=O groups. For the three addition channels on

125 the O of C=O groups in **AB** molecule, the natural charge density on site 2 (-0.33) >
126 site 4 (-0.25) > site 3 (-0.17). As a result, site 2 shows higher reactivity, the reaction
127 potential barrier heights of **AB** on site 2 would be lower than those of the other two
128 reaction site 3 and 4.

129 The calculated imaginary frequencies of nine transition states, the optimized bond
130 lengths for breaking and forming bonds, and the corresponding chemical reaction
131 equations are listed in Table 2. The normal mode analysis confirms that all transition
132 states present a single imaginary frequency which corresponds to the stretching mode
133 of coupling fracture and bond formation. In TSA-1 and TAB-1 structures, it can be
134 seen that the breaking bonds C—H increase by 18.27% and 18.09% compared with
135 the equilibrium bond length in Pe; the forming bonds C—H stretch by 32.18% and
136 32.36% over the equilibrium bond lengths in isolated **A** and **AB**, respectively. The
137 elongation of the breaking bond is smaller than that of the corresponding forming
138 bond, in the case of the three electrophilic addition reaction channels of TSB, TSAB-2
139 and TSA-2, similar features can be drawn, which indicates that the above-mentioned
140 electrophilic addition reactions are all reaction-like, i.e., the five reaction channels
141 will proceed *via* “early” transition states. It is consistent with Hammond’s postulate
142 [28], for an exothermic reaction.

143 **3.2. Frontier MOs and Energetics**

144 Table 3 lists the adiabatic IP (a), EA (a) and the corresponding experimental data [29],
145 as well as the calculated HOMO-LUMO gap (E_g), the value of BP for reference.
146 Compared with Pe, the other molecules in Table 3 all have π bonds. π bond has higher
147 HOMO and lower LUMO compared with σ bond, so the E_g value is relatively lower.
148 Moreover, as the conjugated system increases, the gap between the HOMO and the
149 LUMO keeps narrowing. Therefore, the order of E_g values is: **AB** < **A** < **B** < MAM <

150 BP < Aa < Pe, and **AB** has the lowest E_g value.

151 The σ electrons are in the sp^n hybrid orbits, which are close to the nucleus. The σ
152 electrons can not dissociate easily, as they are firmly attracted by the nucleus. While
153 the π electrons are in the p orbitals, which are far from the nucleus, so they are easier
154 to dissociate than the σ electrons. In a conjugated system, the degree of delocalization
155 of π electrons will increase with the enlarging of the conjugated system, and the
156 degree of being bounded by the nucleus will be lower, so it is easier for π electrons to
157 dissociate from the system. It is reported that compounds containing conjugated
158 aromatic structure are suitable to act as voltage stabilizers [16,17]. The IP values in
159 Table 3 of BP, Aa, **AB**, **A** and **B** are all smaller than Pe, while the IP value of MAM is
160 the highest. The analysis shows that the proportion of heteroatoms in MAM's
161 conjugated chain is 3/7(4 C atoms, 1 N atom and 2 O atoms), which is higher than that
162 of the other conjugated molecules. Compared with C atoms, heteroatoms have the
163 greater electronegativity, so the electrons in MAM are not easy to emit. At the same
164 time, the greater the proportion of electronegative atoms in the molecule is, the easier
165 it is to accept the hot electrons. MAM contains relatively more heteroatoms, so its EA
166 value (1.35 eV) is relatively large, much larger than Pe. It is reported that MAM can
167 be used as space charge inhibitor [14,15]. On the other hand, our researches show that
168 when the conjugated system in the molecule gets larger, its accepting hot electrons'
169 ability gets higher as while, and it is much easier for the larger conjugated system to
170 disperse the accepted hot electrons, so the EA value becomes higher, this regularity
171 can be seen in Table 3 also. In consideration of the above two factors, the EA value of
172 **AB** is the largest.

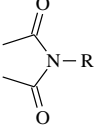
173 As a voltage stabilizer, it needs to have an excellent ability to receive hot electrons,
174 **AB** molecule has it, at the same time, the imine structure in **AB** has the capability of

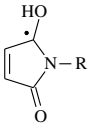
175 space charge suppression. Therefore, it is ideal to select **AB** molecule as a
176 multi-functional additive to improve the electric breakdown strength and inhibit the
177 generation of space charge. We focus on the potential energy surface of the reaction
178 between **AB** molecule and Pe in the following study.

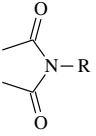
179 The reaction energy barrier (ΔG^\ddagger) and the reaction Gibbs free energy (ΔG^0) for the
180 nine reaction channels are also listed in Table 2. **AB** can be sensitized by
181 photo-initiator BP mentioned above. It can be seen that **AB**, **A** and **B** can be grafted to
182 the Pe chain by UV radiation, moreover, **AB** can be grafted to the Pe chain through
183 four sites. From the data in Table 2, we can also discover that the order of reaction
184 potential barrier (ΔG^\ddagger) of four sites in **AB** is $\Delta G^\ddagger_{\text{site1}}$ (0.89 eV) < $\Delta G^\ddagger_{\text{site2}}$ (1.24 eV)
185 < $\Delta G^\ddagger_{\text{site4}}$ (1.96 eV) < $\Delta G^\ddagger_{\text{site3}}$ (2.05 eV). As for the reaction on site 1, it has the
186 lowest reaction potential barrier among the four reaction channels.

187 For the three electrophilic addition reactions of the 4-position hydrogen in Pe to C of
188 C=O groups (carbonyl in amide, ester carbonyl and ketone carbonyl), the reaction
189 potential barrier on site 3 of **AB** is 2.05 eV, which is the highest among the four
190 reaction sites. Site 2 has the lowest reaction potential barrier (1.24 eV) and the lowest
191 Gibbs free energy ($\Delta G^0 = -0.01$ eV). The reaction channel of site 2 is more
192 advantageous than other channels in thermodynamics and kinetics. In Table 2, we can
193 see that the reaction potential barrier of the grafting of **AB** on site 3 is higher than that
194 on site 2 and site 4, this is consistent with the results of natural charge population
195 discussed above (see Table 4). It can be deduced that with the increasing of charge
196 density of the C=O double bond, the reaction potential barrier of electrophilic addition
197 reaction decreases. In other words, when the charge density of the C=O double bond
198 in the molecule decreases, the electrophilic hydrogen addition reaction will become
199 more and more difficult.

200 Compare the addition reaction on C of C=C group with O of C=O group in **AB**, it can
201 be seen from Table 2 that for the electrophilic addition reaction at 4-position
202 hydrogen in Pe with O of C=O group, a larger conjugated system has not been formed.

203 Because the conjugated structure of the diimide  is destroyed, resulting in a

204 cross conjugated system . The cross conjugated system is weaker than that of
205 the diimide conjugated system, and the corresponding cross conjugated system
206 reaction activity becomes weaker. While for the electrophilic addition reaction of the
207 4-position hydrogen in Pe to C of C=C group, it is just on the opposite. The

208 conjugated structure of diimide  is not broken and the reactivity is enhanced.

209 Thus, $\Delta G^\ddagger(\text{site 1})$ (0.89 eV) < $\Delta G^\ddagger(\text{site 2})$ (1.24 eV). The value of NBO in Table 4
210 exactly illustrates the problem. In experimental study **AB** can be grafted onto the PE
211 chain [18]. According to our computed results, the electrophilic addition reaction of
212 the 4-position hydrogen in Pe to C of C=C group is the dominant reaction channel.
213 **AB** can be used as a potential multi-functional additive of XLPE insulation material.
214 In addition, as aryl cation in **AB** molecule possesses strong ability of π -electron
215 delocalization than that of alkyl cation PE, aromatic molecule **AB** is chosen as an
216 additive added in XLPE composite material, which can restore alkyl cation radical
217 from transforming the alkyl cation radical to relatively stable aryl cation radical.

218 **4. Conclusion**

219 The multiple-channel addition reactions mechanism of hydrogen in polyethylene to
220 four sites on **AB** molecule has been investigated. The electrophilic addition reaction

221 of the 4-position hydrogen in Pe to C of C=C group is more likely to occur than that
222 of the 4-position hydrogen in Pe to O of C=O groups. As a multi-functional additive,
223 **AB** molecule can be grafted onto the PE chain by UV radiation to avoid migration. As
224 a UV absorber, **AB** molecule can play roles as a voltage stabilizer and space electron
225 inhibitor, improve the electronic breakdown strength of PE insulating materials, and
226 inhibit the generation and accumulation of space charges. The use of multi-functional
227 **AB** molecule in the material system will reduce the amount of additives and the
228 introduction of chemical impurities, and improve the electronic conductivity of
229 insulating materials.

230

231 **Acknowledgements**

232 This work is supported by the National Natural Science Foundation of China
233 (51337002) and Key Project of the Joint Fund for Regional Innovation and
234 Development of National Natural Science Foundation of China (U20A2030).

235 **Declaration**

236 **Availability of data and material** The standard coordination of the TSs for every
237 channel is given in the supporting information.

238 **Code availability** The study was carried out on the basis of Gaussian 09, Revision
239 A.01.

240 **Authors' contributions** We declare that this work was done by the authors named in
241 this article, and all liabilities pertaining to claims relating to the content of this article
242 will be borne by the authors. In addition, a declaration of the role of each author
243 mentioned as follows: Prof. Hui Zhang carried out the geometry optimizations,
244 participated in data analysis, and drafted the manuscript; Dr. Chi Deng carried out the
245 calculation of stationary points and frequency analysis; Dr. Xia Du carried out the

246 calculation of charger density and the statistical analysis, collected field data; Prof.
247 Yan Shang participated in the analysis of the results; Prof. Hong Zhao, Xuan Wang
248 and Baozhong Han designed the study; Prof. Zesheng Li helped perform the analysis
249 with constructive discussions. All authors read and approved the final manuscript.
250 **Conflicts of interest** The authors declare no competing interests.

References

- [1] Orton H (2015) Power cable technology review[J]. High Voltage Engineering. 41:1057-1067
- [2] Montanari GC, Laurent C, Teyssedre G, Campus A, Nilsson UH (2005) From LDPE to XLPE: Investigating the change of electrical properties. Part I. space charge, conduction and lifetime[J]. IEEE Trans Dielectr Electr Insul 12: 438-446. <https://doi:10.1109/TDEI.2005.1453448>
- [3] Mazzanti G, Montanari GC, Dissado LA (2005) Electrical aging and life models: the role of space charge[J]. IEEE Trans Dielectr Electr Insul 12: 876-890. <https://doi:10.1109/TDEI.2005.1522183>
- [4] Montanari GC, Mazzanti G, Palmieri F, Motori A, Perego G, Serra S (2001) Space-charge trapping and conduction in LDPE, HDPE and XLPE[J]. J Phys D 34: 2902-2911. <https://doi:10.1088/0022-3727/34/18/325>
- [5] Zhang H, Shang Y, Zhao H, Han BZ, Li ZS (2013) Mechanisms on electrical breakdown strength increment of polyethylene by acetophenone and its analogues addition:a theoretical study[J]. J Mol Model 19: 4477-4485. <https://doi:10.1007/s00894-013-1946-1>
- [6] Zhang H, Shang Y, Li MX, Zhao H, Wang X, Han BZ (2015) Theoretical study on the radical reaction mechanism in the cross-linking process of polyethylene[J]. RSC Adv 5: 90343-90353. <https://doi:10.1039/c5ra16339k>
- [7] Zhang H, Shang Y, Wang X, Zhao H, Han BZ, Li ZS (2013) Mechanisms on electrical breakdown strength increment of polyethylene by aromatic carbonyl compounds addition: a theoretical study[J]. J Mol Model 19: 5429-5438. <https://doi:10.1007/s00894-013-2028-0>
- [8] Yamano Y, Endoh H (1998) Increase in breakdown strength of PE film by

- additives of azocompounds[J]. IEEE Trans Dielectr Electr Insul 5: 270-275.
- [9] Yamano Y (2006) Roles of polycyclic compounds in increasing breakdown strength of LDPE film[J]. IEEE Trans Dielectr Electr Insul 13: 773-781. <https://doi:10.1109/TDEI.2006.1667735>
- [10] Yamano Y, Iizuka M (2009) Suppression of electrical tree initiation in LDPE by additives of polycyclic compound[J]. IEEE Trans Dielectr Electr Insul 16: 189-198. <https://doi:10.1109/TDEI.2009.4784567>
- [11] Jarvid M, Johansson A, Englund V, Gubanski S, Andersson MR (2012) Electrical treeing Inhibition by Voltage Stabilizers, Annual Report Conference on Electrical Insulation and Dielectric Phenomena, 605-608
- [12] Lee SH, Park JK, Han JH, Suh KS (1997) Space charge behavior in maleic anhydride grafted polyethylene/ethylene-vinyl-acetate copolymer laminates[J]. J Phys D Appl Phys 30:1. <https://doi:10.1088/0022-3727/30/1/001>
- [13] Lee SH, Park JK, Han JH, Suh KS (1995) Space charge and electrical conduction in maleic anhydride-grafted polyethylene[J]. IEEE Trans Dielectr Electr Insul 2: 1132-1139. <https://doi:10.1109/TDEI.1995.8881931>
- [14] Zhang H, Shang Y, Zhao H, Li CY, Wang X, Han BZ, Li ZS (2018) Theoretical study on the grafting reaction of maleimide to polyethylene in the UV radiation cross-linking process[J]. Polymers 10: 1044. <https://doi:10.3390/polym10091044>
- [15] Wang Y, Zhang H, Zhao H, An T, Du X, Lu Y, Chen ZG (2019) Theoretical study on the grafting reaction of maleimide and its derivatives to polyethylene in the UV radiation cross-linking process[J]. Struct Chem 30: 1033-1039. <https://doi:10.1007/s11224-018-1250-x>
- [16] Zhang H, Shang Y, Zhao H, Wang X, Han BZ, Li ZS (2016) Theoretical study on

- the tailored side-chain architecture of benzil-like voltage stabilizers for enhanced dielectric strength of cross-linked polyethylene[J]. RSC Adv 6: 11618. <https://doi:10.1039/c5ra23718a>
- [17] Zhang H, Zhao H, Wang X, Shang Y, Han BZ, Li ZS (2014) Theoretical study on the mechanisms of polyethylene electrical breakdown strength increment by the addition of voltage stabilizers. J Mol Model 20: 2211. <https://doi:10.1007/s00894-014-2211-y>
- [18] Na HS, Kim TH (2014) Grafting of maleimide containing 2-hydroxy-benzophenone onto polyethylene: reaction conditions and photo-stabilization effects. Macromol Res 22: 958-962. <https://doi:10.1007/s13233-014-2133-7>
- [19] Parr RG, Yang W (1989) Density-Functional Theory of Atoms and Molecules, Oxford University Press, New York, NY, USA
- [20] Truong TN, Duncan WT, Bell RL (1996) Chemical Applications of Density Functional Theory, vol. 85, American Chemical Society, Washington, DC, USA, ISBN 0-8412-3403-5
- [21] Lee C, Yang W, Parr RG (1988) Development of the Colle-Salvetti correlation energy formula into a functional of the electron density. Phys Rev B 37: 785-789, <https://doi.org/10.1103/PhysRevB.37.785>
- [22] Miehlich B, Savin A, Stoll H, Preuss H (1989) Results obtained with the correlation energy density functionals of Becke and Lee, Yang and Parr. Chem Phys Lett 157: 200-206. [https://doi.org/10.1016/0009-2614\(89\)87234-3](https://doi.org/10.1016/0009-2614(89)87234-3)
- [23] Becke AD (1993) Density-functional thermochemistry. III. The role of exact exchange. J Chem Phys 98: 5648-5652. <https://doi.org/10.1063/1.464913>
- [24] Zangwill A, Soven P (1980) Density-functional approach to local-field effects

- infinite systems-photoabsorption in the rare-gases. Phys Rev A 21:1561-1572.
<https://doi.org/10.1103/PhysRevA.21.1561>
- [25] Levine ZH, Soven P (1984) Time-dependent local-density theory of dielectric effects in small molecules. Phys Rev A 29: 625-635.
<https://doi.org/10.1103/PhysRevA.29.625>
- [26] Reed AE, Weinstock RB, Weinhold F (1985) Natural population analysis. J Chem Phys 83: 735-746. <https://doi.org/10.1063/1.449486>
- [27] Frisch J, Trucks GW, Schlegel HB, Scuseria GE, Robb MA, Cheeseman JR, Scalmani G, Barone V, Mennucci B, Petersson GA, et al. (2010) Gaussian 09 Revision B.01, Gaussian Inc., Wallingford CT
- [28] Hammond GS (1955) J Am Chem Soc 77: 334.
- [29] Lias SG, Levin RD, Kafafi SA, Bartmess JE, NIST ChemistryWebBook, NIST standard reference database number 69. <https://webbook.nist.gov/chemistry/>

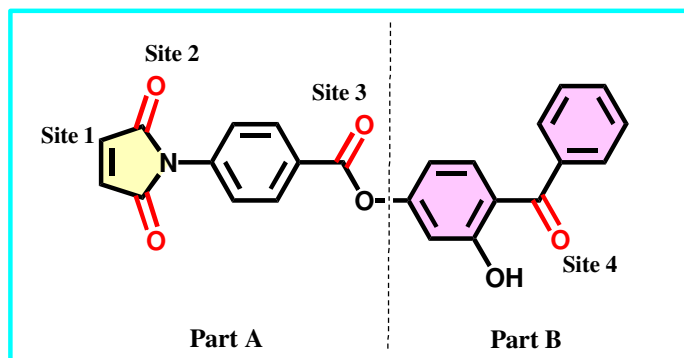


Figure 1 Schematic diagram of molecular structure of **AB**

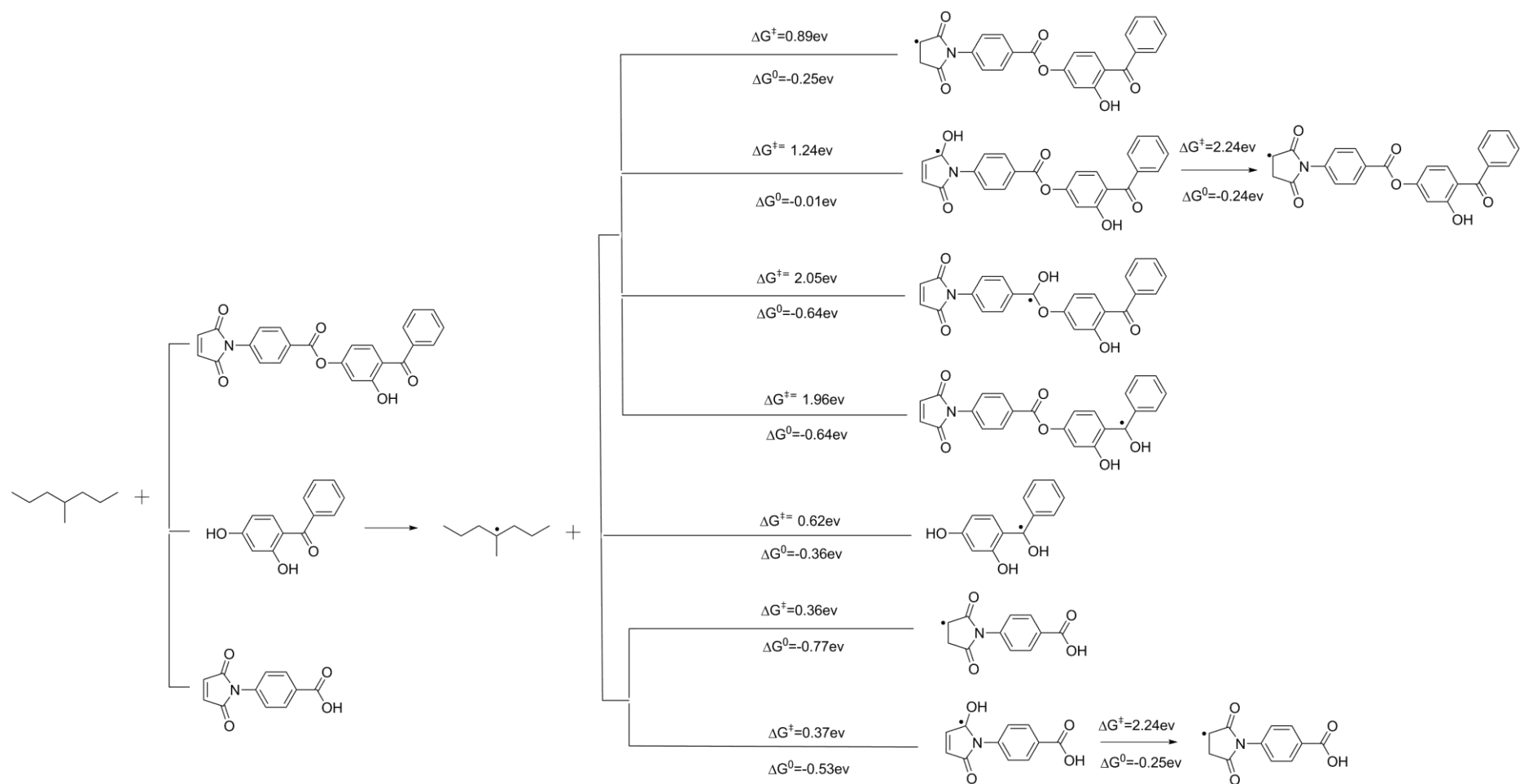


Figure 2 The schematic diagram of reaction progress of the studied nine channels

Table 1 The molecular name, the molecular formula, and corresponding abbreviation (ab.) of the studied molecules.

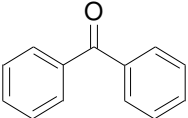
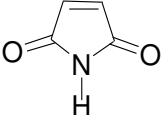
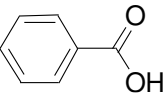
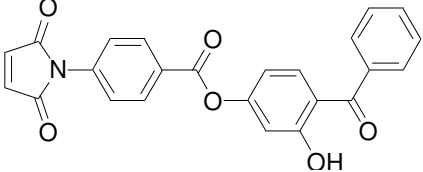
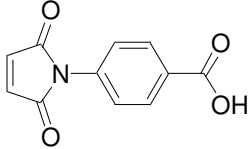
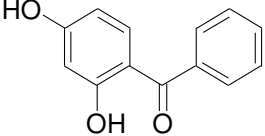
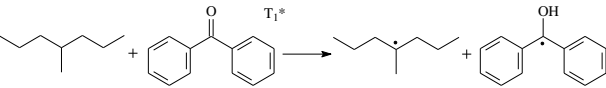
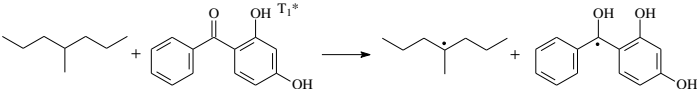
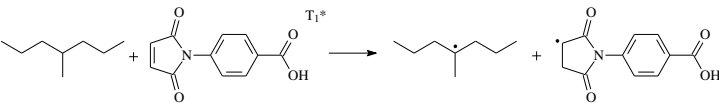
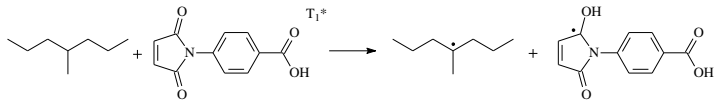
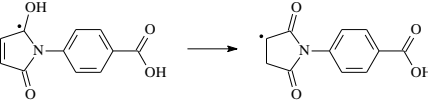
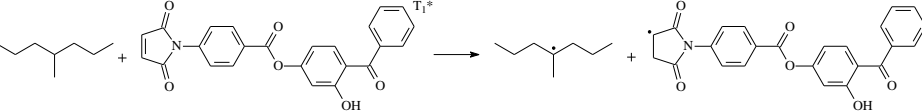
ab.	Molecular Formula	Molecular Name
Pe		4-methylheptane
BP		benzophenone
MAM		maleimide
Aa		benzoic acid
AB		4-(2,5-dioxo-2,5-dihydro-pyrrol-1-yl)- benzoic acid-4-benzoyl 3-hydroxy-phenyl ester
A		4-(2,5-dioxo-2,5-dihydro-pyrrol-1-yl) benzoic acid
B		2,4-dihydroxybenzophenone

Table 2 Optimized bond lengths of breaking/forming bonds for transition state, reactants and products (in angstrom), together with the calculated breaking/forming bond frequencies (in cm^{-1}), the reaction energy barrier (ΔG^\ddagger) and reaction Gibbs free energies ΔG^0 (in eV), as well as the abbreviation of transition state (ab.).

reaction equation	reactant	b/f	product	freq.	ΔG^\ddagger	ΔG^0	ab.
	1.100	1.228/1.395	0.964	835 <i>i</i>	0.60	-0.46	TSBP
	1.100	1.239/1.375	0.965	1156 <i>i</i>	0.62	-0.36	TSB
	1.100	1.301/1.450	1.097	1198 <i>i</i>	0.36	-0.77	TSA-1
	1.100	1.192/1.496	0.964	334 <i>i</i>	0.37	-0.53	TSA-2
	0.964	1.382/1.505	1.097	2010 <i>i</i>	2.24	-0.25	TSA-3
	1.100	1.299/1.452	1.097	1182 <i>i</i>	0.89	-0.25	TSAB-1

	1.100	1.192/1.500	0.964	329 <i>i</i>	1.24	-0.01	TSAB-2
	0.964	1.382/1.504	1.097	2011 <i>i</i>	2.24	-0.24	TSAB-5
	1.100	1.445/1.162	0.966	1654 <i>i</i>	2.05	0.64	TSAB-3
	1.100	1.225/1.403	0.969	833 <i>i</i>	1.96	0.64	TSAB-4

Table 3 The E_g , IPs, and EAs of studied molecules calculated as well as the corresponding experimental data in the bracket (in eV).

ab.	molecular formula	E_g	IP(<i>a</i>)	EA(<i>a</i>)
Pe		8.38	9.41	-1.09
BP		4.90	8.64(9.05)	0.73(0.69 ± 0.05)
MAM		4.78	10.22	1.35
Aa		5.65	9.30(9.30)	0.23
AB		3.28	7.91	2.00
A		3.92	8.55	1.86
B		4.60	7.80	0.46

Table 4 Natural charges population analysis of four sites on T_1 state of **AB** molecule.

	Natural Charges Population			
	1	2	3	4
T_1	-0.140	-0.330	-0.167	-0.254

Figures

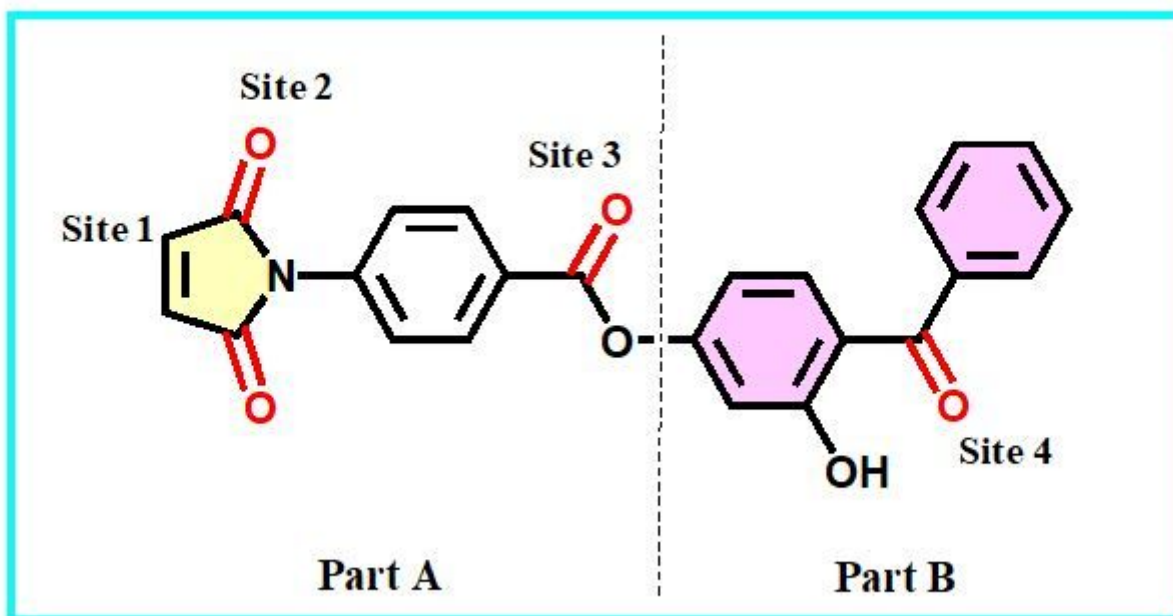


Figure 1

Schematic diagram of molecular structure of AB

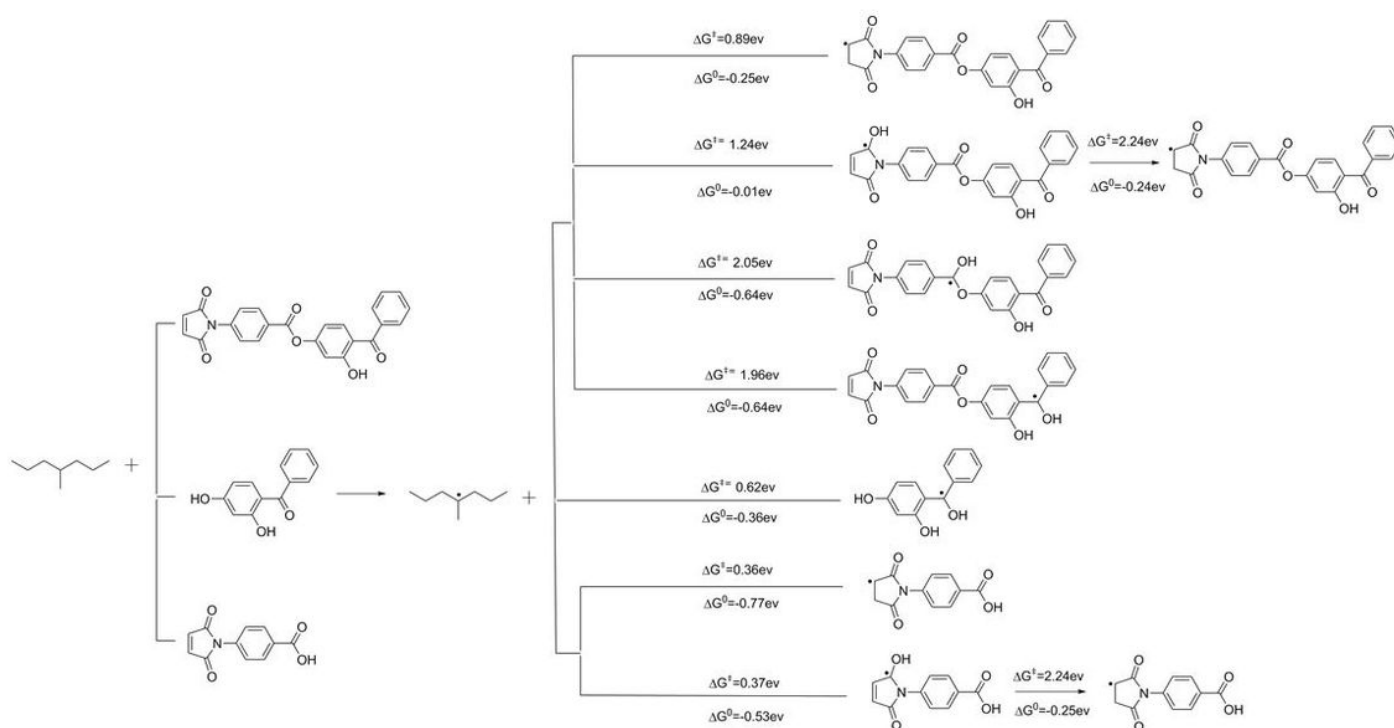


Figure 2

The schematic diagram of reaction progress of the studied nine channels

Supplementary Files

This is a list of supplementary files associated with this preprint. Click to download.

- [graphicalabstract.jpg](#)
- [supportinginformation.doc](#)